PRAMANA
— journal of
physics

Vol. 75, No. 4
October 2010
pp. 737–748

Molecular dynamics of liquid alkaline-earth metals near the melting point

J K BARIA[1,*] and A R JANI[2]
[1]Department of Physics, V.P. & R.P.T.P. Science College, Vallabh Vidyanagar 388 120, India
[2]Department of Physics, Sardar Patel University, Vallabh Vidyanagar 388 120, India
*Corresponding author. E-mail: jay_baria@yahoo.com

MS received 14 January 2010; accepted 22 April 2010

Abstract. Results of the studies of the properties like binding energy, the pair distribution function $g(r)$, the structure factor $S(q)$, specific heat at constant volume, velocity autocorrelation function (VACF), radial distribution function, self-diffusion coefficient and coordination number of alkaline-earth metals (Be, Mg, Ca, Sr and Ba) near melting point using molecular dynamics (MD) simulation technique using a pseudopotential proposed by us are presented in this article. Good agreement with the experiment is achieved for the binding energy, pair distribution function and structure factor, and these results compare favourably with the results obtained by other such calculations, showing the transferability of the pseudopotential used from solid to liquid environment in the case of alkaline-earth metals.

Keywords. Molecular dynamics; pair distribution function; structure factor; binding energy; velocity autocorrelation function.

PACS Nos 61.20.Lc; 61.25.Mv; 71.15.Pd; 71.15.Dx

1. Introduction

The alkaline-earth metals (IIA column) can be considered as simple metals electronically and they are certainly the less studied elements among the metals. From the experimental point of view, only a few properties such as the electrical resistivity [1], the absolute thermopower [2], the static structure [3], the sound velocity [4] and the density [5] have been determined so far. This is because of the high chemical reactivity and gas adsorption ability [6] that further increase with temperature. Because of these difficulties, technologically and theoretically alkaline-earth metals were not interesting, while alkali and polyvalent ones were often preferred. However, alkaline-earth metals have a central place. On the one hand, they can be considered as simple and free-electron-like, as they have only s-like conduction electrons. Beryllium and magnesium, essentially free-electron-like, are as simple as sodium [7]. But, in Ca, Sr and Ba, the existence of an empty d-band above the Fermi level, which get nearer as one goes down the IIA column [8] has a great

influence on the electronic properties. This explains the high electrical resistivity of liquid barium [1,9].

Recent works [8,10–12] have been devoted to this class of elements to see trends through the Periodic Table and to study the transition from alkali to more complex metals in relation to the influence of the electron gas. Alemany *et al* [12] also computed the velocity autocorrelation function (VACF), its memory function and the self-diffusion coefficient.

In this paper, we study properties like binding energy, the pair distribution function $g(r)$, the structure factor $S(q)$, specific heat at constant volume, velocity autocorrelation function (VACF), radial distribution function, self-diffusion coefficient and coordination number using molecular dynamics (MD) simulation technique with a pseudopotential of Baria and Jani [13–15] for alkaline-earth metals, namely beryllium, magnesium, calcium, strontium and barium. We present the results of the static properties i.e., binding energy, the structure factor and the pair distribution function and compare them with both experimental and theoretical works done previously, as well as the VACF and its spectral density. Because of the lack of experimental data for VACF, we could compare our results only with the recent ones of Alemany *et al* [12]. Our calculations have been performed with the molecular dynamics simulation technique using the pseudopotential of Baria and Jani [13–15] in the second-order perturbation theory.

2. Theory

Simple metals are usually depicted as an assembly of ions of well-defined electric charge immersed in the bath of the conduction electrons, the global system being electrically neutral. As the number of conduction electrons per atom has an integer value ($Z = 2$ for alkaline-earth metals), the direct ion–ion repulsion, essentially Coulombic, is easy to describe contrary to the transition metals. In contrast, the description of the effective ion–ion interaction is drastically affected by the electron–electron and the electron–ion interactions.

The electron–electron interaction relies on the electronic charge density, which takes a well-defined value for simple metals. Its description is done in terms of screening with two functions, the Lindhard–Hartree dielectric function $\varepsilon_{\mathrm{H}}(q)$ and the local-field correction $G(q)$, which account for electrostatic and exchange-correlation effects, respectively. Wax and Bretonnet [16] have shown that the important characteristic of $G(q)$ at least for the static structure factor of liquid metals is the low-q limit parameter depending on the correlation energy of the electron gas. The exchange-correlation effect is nowadays well-predicted by Monte Carlo techniques, and the Ichimaru and Utsumi [17] IU expression of the local-field correction used in this work is certainly one of the most reliable.

Since alkaline-earth metals are simple like metals, the main difficulty in the calculation of the effective ion–ion interaction lies in the description of the electron–ion interaction. Thus, the effective pair potential can be obtained from the perturbation theory applied to second order for the determination of the configurational energy of the material,

$$u(r) = \frac{Z^2}{r} - \frac{2Z^2}{\pi} \int_0^\infty F_{\mathrm{N}}(q) \frac{\sin(qr)}{qr}\, \mathrm{d}q. \tag{1}$$

Table 1. Input parameters, binding energy (in Ryd.) and specific heat at constant volume. The value in parentheses shows the percentage deviation of the binding energy from the experimental findings.

Element	T (K)	$\Omega(a_0^3)$	r_c (a.u.)	r_s	$(3/2)k_B T$	E_{vol}	E_{con}	$E_{bin}^{present}$	E_{bin}^{expt} [22]	C_V^* (a.u.)
Be	1560	59.82	0.92411	1.9274	0.01482	−2.4275	0.1016	−2.3110 (1.91%)	−2.2676	3.67
Mg	980	173.20	1.66547	2.7445	0.00931	−1.8040	0.0325	−1.7621 (1.11%)	−1.7820	3.90
Ca	1138	333.03	2.88390	3.4128	0.01081	−1.5069	0.0569	−1.4391 (2.02%)	−1.4688	2.98
Sr	1040	420.38	3.21860	3.6884	0.00988	−1.3816	0.0456	−1.3261 (2.08%)	−1.3544	3.21
Ba	998	465.12	3.35410	3.8148	0.00948	−1.3390	0.0239	−1.3056 (4.24%)	−1.2524	2.98

$F_N(q)$ is the normalized energy-wave number characteristic which is given by

$$F_N(q) = \left(\frac{q^2 V}{4\pi Z N}\right)^2 \left[1 - \frac{1}{\varepsilon(q)}\right] \left(\frac{1}{1 - G(q)}\right) |W_B(q)|^2, \tag{2}$$

where $V/N = \Omega_0$, is the atomic volume, $\varepsilon(q)$ is the electron-gas dielectric function and $G(q)$ is the local-field correction that takes into account the exchange-correlation effects [17] between conduction electrons. $W_B(q)$, the pseudopotential proposed by Baria and Jani [13–15] (in Ryd. Unit) is given by

$$W_B(q) = -\frac{8\pi Z}{\Omega_0 q^2} \left\{ \begin{array}{l} \dfrac{4(\cos(qr_c) - 1)}{q^2 r_c^2} + \dfrac{4\sin(qr_c)}{qr_c} \\ + \dfrac{\sin(qr_c)}{(1 + q^2 r_c^2)^3} [5qr_c - 4q^3 r_c^3 - q^5 r_c^5] \\ + \dfrac{\cos(qr_c)}{(1 + q^2 r_c^2)^3} \left[11q^2 r_c^2 + 4q^4 r_c^4 + q^6 r_c^6\right] \\ + \dfrac{2eq^2 r_c^2 (q^2 r_c^2 - 3)}{(1 + q^2 r_c^2)^3} - \cos(qr_c) \end{array} \right\}, \tag{3}$$

where r_c is the potential parameter and e is the base of natural logarithm. We have calculated the parameter of the potential r_c using standard zero pressure technique. The corresponding parameters are compiled in table 1. Another variable aspect of the pseudopotential formalism is the choice of the exchange-correlation function, $G(q)$. We employ the expression exempt from free parameters, which was developed by Ichimaru and Utsumi [17].

In the framework of the second-order perturbation theory of the pseudopotential, the binding energy is given by the energy of an atom as,

$$E_{bin} = \frac{3}{2} k_B T + E_{con} + E_{vol}. \tag{4}$$

The configurational energy $E_{\rm con}$ is obtained directly by molecular dynamics or from its definition in terms of pair distribution function $g(r)$,

$$E_{\rm con} = \frac{N}{2V} \int u(r)\, g(r)\, {\rm d}r. \tag{5}$$

The volume-dependent contribution to the binding energy, $E_{\rm vol}$, is given according to the prescription of Hasegawa and Watabe [18] as

$$E_{\rm vol} = E_{\rm eg} - \lim_{q\to 0} \left[2\pi Z^2 \frac{N}{V} \left(\frac{\pi}{4k_{\rm F}} - \frac{G(q)}{q^2} \right) \right] - \frac{1}{2V} \sum_{q\neq 0} \frac{4\pi Z^2}{q^2} F_{\rm N}(q) = E_{\rm eg} + B_{\rm eg} + \Phi. \tag{6}$$

In this expression, $E_{\rm eg}$ represents the ground state energy of the electron gas, for which the following Nozieres-Pines [19] interpolation formula is used (within atomic units):

$$E_{\rm eg} = \frac{Z}{2} \left[\frac{2.21}{r_{\rm s}^2} - \frac{0.916}{r_{\rm s}} + 0.031 \, \ln(r_{\rm s}) - 0.115 \right], \tag{7}$$

where $r_{\rm s}$ is the radius of the electronic sphere defined by $r_{\rm s}^3 = \frac{9\pi}{4k_{\rm F}^3} = \frac{3}{4\pi} \left(\frac{V}{NZ} \right)$. The first term of eq. (7) is the kinetic energy of the free electron gas, the second term is the attractive exchange energy due to the parallel-spin electrons separated by Pauli's exclusion principle and the third term is the correlation energy that gives an additional lowering in energy.

In the right-hand side of eq. (6), the second term, usually noted as $B_{\rm eg}$, corresponds to a rearrangement of various energetic contributions for the zero-wave vector and the third term noted as Φ, represents the self-energy between an ion and its surrounding cloud of charge. In this context, the local pseudopotential assumed for the ion–electron interaction and the local-field correction $G(q)$ considered for the exchange and correlation effects within the electron gas are crucial for obtaining the volume-dependent energy.

3. Molecular dynamics simulation

The molecular dynamics (MD) simulations are performed in the NVE microcanonical ensemble. The system is a cubic box containing Natoms with periodic boundary conditions and the box sizes are fitted to the desired density, $\rho = N/V = 1/\Omega_0$. During the thermalization stage, the system relaxes and the velocities are rescaled each 50 time steps to the expected temperature. Once the system is thermalized, the production stage is launched and positions and velocities of the particles are taped each 5 (for dynamical properties) or 10 (for static ones) time steps. During this stage, the temperature is no more renormalized. Because of the statistical fluctuations, for which standard deviations of the temperature are a few tenths of degrees, the effective temperature during the production differs from the expected one.

In this paper, we are indicating the effective value of the temperature at which the results are obtained, because as will be seen later, the self-diffusion coefficient is highly sensitive to the temperature. It is worth mentioning that the isothermal MD simulation, which requires the renormalization of the velocities, is prescribed to observe the evolution of a tagged particle in order to compute the VACF. Depending on the physical properties under study, two different sizes for the simulation box are used; 256 particles for dynamical properties and 2048 particles for static properties. The bigger is the system, the faster is the thermalization and the smaller are the fluctuations of the temperature.

Knowing a great number of successive configurations, the pair distribution function $g(r)$ can be determined from the relationship,

$$g(r) = \frac{n(r)}{(4/3)\pi\rho C[(r+\delta r)^3 - r^3]}, \tag{8}$$

where C is the number of configurations taped and $n(r)$ is the number of atoms counted at a distance between r and $r + \delta r$ from another atom taken as origin. As we said, for computing the static structure the box contains $N = 2048$ atoms in order to ensure a large enough r extension of $g(r)$. So, the structure factor $S(q)$ is obtained directly by Fourier transform as

$$S(q) = 1 + \rho \int [g(r) - 1] \exp(-q \cdot r)\, \mathrm{d}r. \tag{9}$$

Another function $4\pi\rho r^2 g(r)$ obtained from $g(r)$ is used for discussing the structure of non-crystalline systems. This is called the radial distribution function (RDF). This function corresponds to the number of atoms in the spherical shell between r and $r + \mathrm{d}r$, the coordination number, and is obtained from the relation [20]

$$n_1 = \int_{r_0}^{r_\mathrm{m}} 4\pi\rho r^2 g(r)\, \mathrm{d}r, \tag{10}$$

where r_0 is the left-hand edge of the first peak and r_m corresponds to the first minimum on the right-hand side of the first peak in RDF.

The determination of the VACF, i.e., $\psi(t)$, requires larger time ranges but smaller systems than for the determination of $S(q)$. In that case, simulations are performed on large time-scales with only N =256 atoms and the VACF is obtained using the following relation:

$$\psi(t) = \frac{1}{N} \lim_{\tau\to\infty} \frac{1}{\tau} \int_0^\tau \sum_{i=1}^{N} V_i(t_0) \cdot V_i(t_0 + t)\, \mathrm{d}t_0. \tag{11}$$

If $\psi(t)$ is known on a time range large enough, the spectral density of the VACF is simply the Fourier transform,

$$\tilde{\psi}(\omega) = \int_{-\infty}^{+\infty} \psi(t) \exp(-i\omega)\, \mathrm{d}t. \tag{12}$$

For the systems under study, it is found that computing $\psi(t)$ on a 2 ps interval is sufficient because beyond this limit the results are dominated by statistical noise.

From phenomenological theory, the self-diffusion coefficient D is related to the spectral density as

$$D = \frac{1}{6}\tilde{\psi}(\omega = 0) = \frac{1}{6}\int_{-\infty}^{+\infty} \psi(t)\,\mathrm{d}t. \tag{13}$$

This relationship provides the connection between the microscopic correlation function and the macroscopic dynamics. Nevertheless, if the configurational evolution is referred to as Brownian motion, D can also be obtained in another way from the mean square displacement ratio (MSDR)

$$\sigma(t) = \frac{1}{N}\lim_{\tau\to\infty}\frac{1}{\tau}\int_0^{\tau}\sum_{i=1}^{N}[r_i(t_0)\cdot r_i(t_0+t)]^2\,\mathrm{d}t_0 \tag{14}$$

because

$$D = \lim_{\tau\to\infty}\frac{\sigma(t)}{6t}. \tag{15}$$

The mean square displacement is a linear function of time and any deviation from linearity must represent some departure from a purely random evolution in the diffusive motion of the particle from its original location. It is a stringent test to determine whether the simulated system is fluid or not. Indeed, if the system is solid, $\sigma(t)$ is quite constant on the time range considered and its mean value is much smaller than the square of the interatomic distance because of the lack of diffusion. The well-suited MD technique for the description of $\sigma(t)$ requires a time range (about 30 ps) larger than that for the VACF. So, production stages of 40,000 time-steps are used for the determination of the dynamical properties. Equations (13) and (15) provide us with a means to check the quality of our calculations as both the values of D should be the same. As can be seen from the results, this equality is verified within 5% in most cases.

The quality of the spectral density can also be assessed by the relation

$$\frac{1}{6\pi}\int_{-\infty}^{+\infty}\tilde{\psi}(\omega)\,\mathrm{d}\omega = \frac{k_{\mathrm{B}}T}{M}, \tag{16}$$

M being the mass of a particle. This relation is verified within 1%.

4. Results and discussion

To determine the binding energy by eq. (7), we first calculate the configurational internal energy E_{con} by MD simulation. We also take advantage of the fluctuations in this energy during the course of the calculation to evaluate the specific heat at constant volume using the standard expression [21]

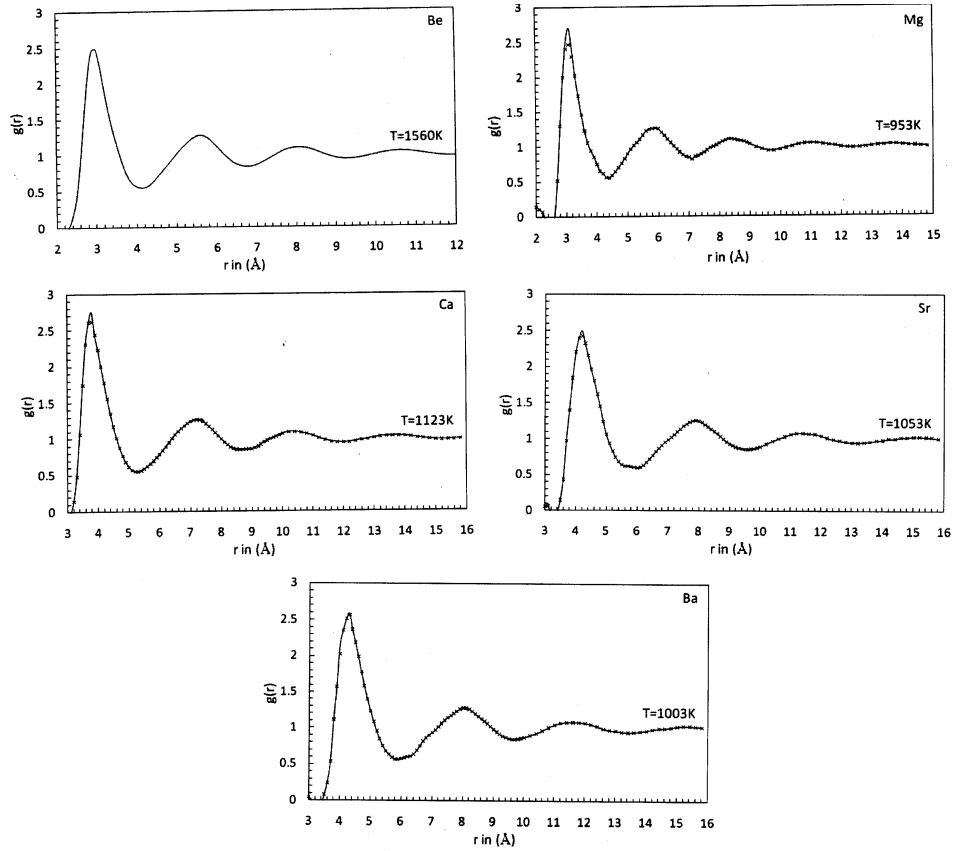

Figure 1. Pair distribution function $g(r)$ for Be, Mg, Ca, Sr and Ba near melting temperature. Full lines are our molecular dynamics results. Crosses ($\times$) are the experimental results of Waseda [20].

$$C_{\mathrm{V}}^{*} = \frac{C_{\mathrm{V}}}{Nk_{\mathrm{B}}} = \frac{3}{2}\left[1 - \frac{3N\langle(\delta E_{\mathrm{con}})^2\rangle}{2\langle E_{\mathrm{kin}}\rangle^2}\right]^{-1}, \tag{17}$$

where $\langle E_{\mathrm{kin}}\rangle$ is the average kinetic energy and δE_{con} is the fluctuation in the configurational energy. Table 1 presents potential parameter r_c, C_{V}^{*} and E_{con} with the other contribution to the volume-dependent energy, as well as the experimental binding energy [22]. Note that the main contribution, Φ, to the binding energy comes from the electrostatic interaction between an ion and its own screening cloud of electrons. Our present values of binding energies are in good agreement with the experimental values within the percentage deviation of 1.11 to 4.24%.

As a test of transferability of the pseudopotential under study, we can compare the binding energy with experiment since it corresponds to the sum of the ionization energies of the valence electrons, E_{ion}, and the cohesive energy, E_{coh}. Indeed, we recall that the conventional binding energy can be written [23] as

$$E = -(E_{\mathrm{ion}} + E_{\mathrm{coh}}). \tag{18}$$

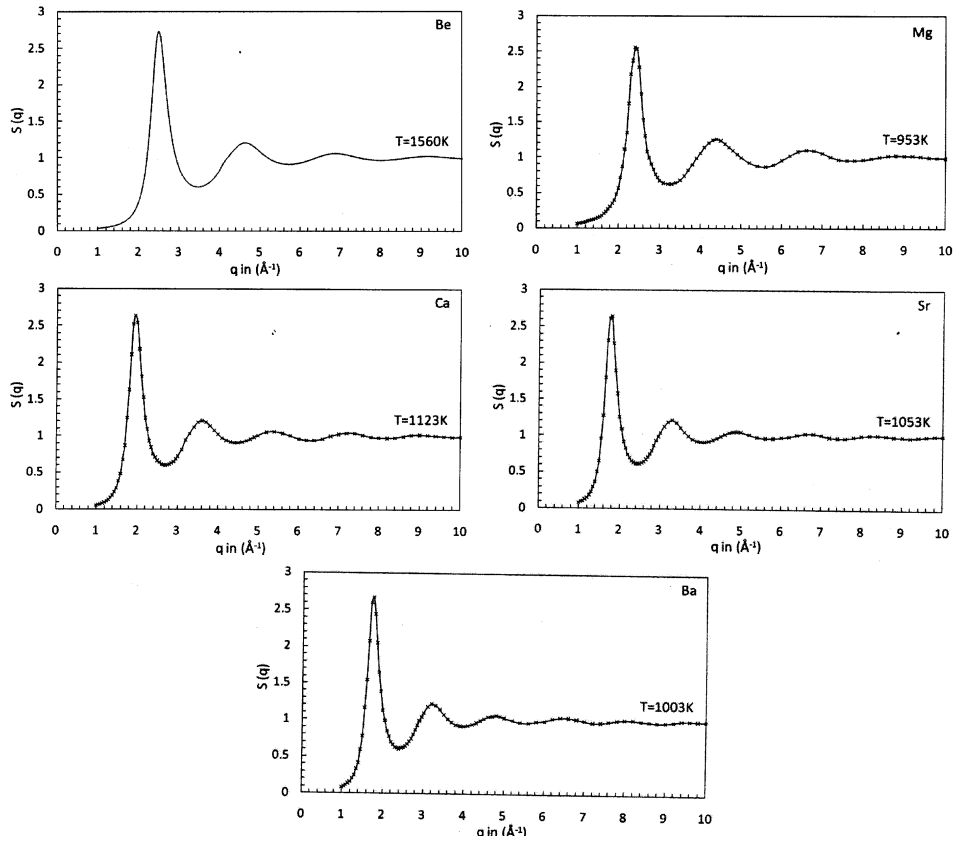

Figure 2. Structure factor $S(q)$ for Be, Mg, Ca, Sr and Ba near melting temperature. Full lines are our molecular dynamics results. Crosses ($\times$) are the experimental results of Waseda [20].

Our results for the pair distribution function $g(r)$ are presented in figure 1 for Be, Mg, Ca, Sr and Ba near their melting points in comparison to the experiments [20]. To our knowledge, no experimental results have ever been published for Be. For Mg, Ca, Sr and Ba, there is a slight overestimation of the height of the first peak with the experimental values of Waseda [20]. Except this, our present findings are excellent.

The corresponding static structure factors $S(q)$ are displayed in figure 2. Though our calculations are performed with 2048 particles, we can see that the low-q behaviour of $S(q)$ is poorly described because of the smallness of the simulation box. The mesh in the q space being governed by the extension of $g(r)$, it may happen that the curves of $S(q)$ are not smooth in some crucial ranges, like the position of the main peak, due to the lack of points. Thus, for Mg, Ca and Ba, the height of the first peak of $S(q)$ seems to be slightly underestimated. Except these small differences, the agreement between our calculations and experiments [20] is overall very satisfactory. The first and second peak positions and their relative magnitudes

Table 2. First and second peak positions of $g(r)$, and their related magnitudes with the coordination number.

Metal	T (K)	First peak position and related magnitude of $g(r)$				Second peak position and related magnitude of $g(r)$				Coordination number n_1	
		First peak position r_1 (Å)		Related magnitude		Second peak position r_2 (Å)		Related magnitude			
		Present	Expt.	Present	Expt.	Present	Expt.	Present	Expt.	Present	Expt.
Be	1560	3.0	–	2.484	–	5.6	–	1.277	–	10.1	–
Mg	953	3.1	3.21	2.701	2.294	6.1	6.0	1.240	1.252	11.2	10.9
Mg	1063	3.1	3.21	2.503	2.144	6.1	6.0	1.203	1.228	11.1	–
Mg	1153	3.1	3.21	2.411	2.126	6.1	6.0	1.186	1.208	11.0	–
Ca	1138	3.8	3.83	2.751	2.614	7.4	7.3	1.264	1.243	11.2	11.1
Sr	1040	4.2	4.23	2.510	2.421	7.9	8.0	1.240	1.248	11.2	11.1
Ba	998	4.3	4.31	2.582	2.561	8.2	8.1	1.260	1.276	10.9	10.8

of $g(r)$, and coordination numbers are shown in table 2 while first and second peak positions and their relative magnitudes of $S(q)$ are shown in table 3. Presently calculated values of the first and second peak positions of $g(r)$, coordination numbers and $S(q)$ excellently agree with the experimental findings of Waseda [20] for Mg, Ca, Sr and Ba while for Be, no experimental data are available for comparison.

In figure 3, we present the VACF for the five alkaline-earth metals in the liquid state at their melting temperatures. The curves exhibit the qualitative feature of the dense fluids with a negative region that is interpreted as the motion of ions in the opposite direction to that they had at $t = 0$. The correlation between the velocities is lost when the VACF reaches zero, its large time limit. In less dense systems, such backscattering is not statistically observed, and it is well known that this decrease obeys a $t^{-2/3}$ law in the case of hard spheres [24] or Lennard–Jones fluids [25].

In liquid state, the global outline of the VACF is the same for all the elements under study. The oscillations, typical of liquid metals [26], are quickly damped and their exact shapes are then blurred by statistical noise. If we consider the results obtained with the neutral pseudoatom method [12], the position of the first minimum is similar to ours, but the depth is increasing with the mass of the atoms. This is not the case for the results of Gupta *et al* [27] obtained with Ashcroft's potential [10]. Gupta *et al* [27] did not use the MD simulation and so the comparison must be drawn with caution. From our results, we also observe that the heavier are the atoms, the slower is the loss of the correlation. Such a relaxation effect must be related to the velocity of the particles, which is higher for lighter atoms. A simple picture would be that a light atom colliding with the neighbouring atoms forms a cage around it more rapidly than a heavier atom.

For the spectral density, $\tilde{\psi}(\omega)$, of the VACF, the low-frequency limit $\tilde{\psi}(\omega = 0)$ is related to the self-diffusion coefficient according to eq. (13). The features that distinguish $\tilde{\psi}(\omega)$ of a liquid from that of an ideal harmonic crystal are the

Table 3. First and second peak positions of $S(q)$, and their related magnitudes.

Metal	T (K)	First peak position and related magnitude of $S(q)$				Second peak position and related magnitude of $S(q)$			
		First peak position q_1 (Å)		Related magnitude		Second peak position q_2 (Å)		Related magnitude	
		Present	Expt.	Present	Expt.	Present	Expt.	Present	Expt.
Be	1560	2.45	–	2.595	–	4.45	–	1.132	–
Mg	953	2.40	2.42	2.501	2.556	4.41	4.40	1.301	1.252
Mg	1063	2.40	2.42	2.356	2.381	4.41	4.40	1.223	1.213
Mg	1153	2.40	2.42	2.239	2.228	4.41	4.40	1.199	1.179
Ca	1138	1.94	1.95	2.630	2.634	3.62	3.63	1.191	1.211
Sr	1040	1.77	1.78	2.650	2.643	3.31	3.30	1.222	1.208
Ba	998	1.75	1.73	2.600	2.661	3.22	3.21	1.198	1.213

Table 4. Self-diffusion coefficients D_ψ and D_σ obtained from eqs (13) and (15) at temperatures T, and the values are obtained from the VACF and the MSDR respectively. The values of D_ψ and D_σ obtained by Alemany *et al* [12] for temperatures are slightly different. The coefficients are given in $Å^2$/ps.

Element	Present			Others [12]			Others [12]		
	T (K)	D_ψ	D_σ	T (K)	D_ψ	D_σ	T (K)	D_ψ	D_σ
Be	1565	0.758	0.785	1565	0.768	0.790	1599	1.041	1.046
Mg	970	0.443	0.479	970	0.440	0.476	1001	0.537	0.517
Ca	1127	0.987	1.024	1127	0.983	1.031	1104	0.625	0.581
Sr	1029	0.549	0.579	1029	0.559	0.572	1038	0.391	0.403
Ba	986	0.469	0.477	986	0.472	0.479	1006	0.329	0.335

widening of the spectrum and the nonzero value at zero frequency. The variation of the spectral density shows that the diffusion increases at melting. When the temperature is further grown, both the diffusion and the vibrations increase with the thermal agitation. The self-diffusion coefficient D can be obtained either from the VACF according to eq. (13) or from the MSDR with eq. (15). The results are summarized in table 4, but the lack of experimental data prevents us from any discussion of their relevance. Even if the order of magnitude of D is acceptable, some remarks have to be done.

5. Conclusion

It is rather difficult to estimate the error for the dynamical properties in computer simulations because many factors influence the results of the calculations. These are the relatively small number of particles, the periodic boundary conditions, the

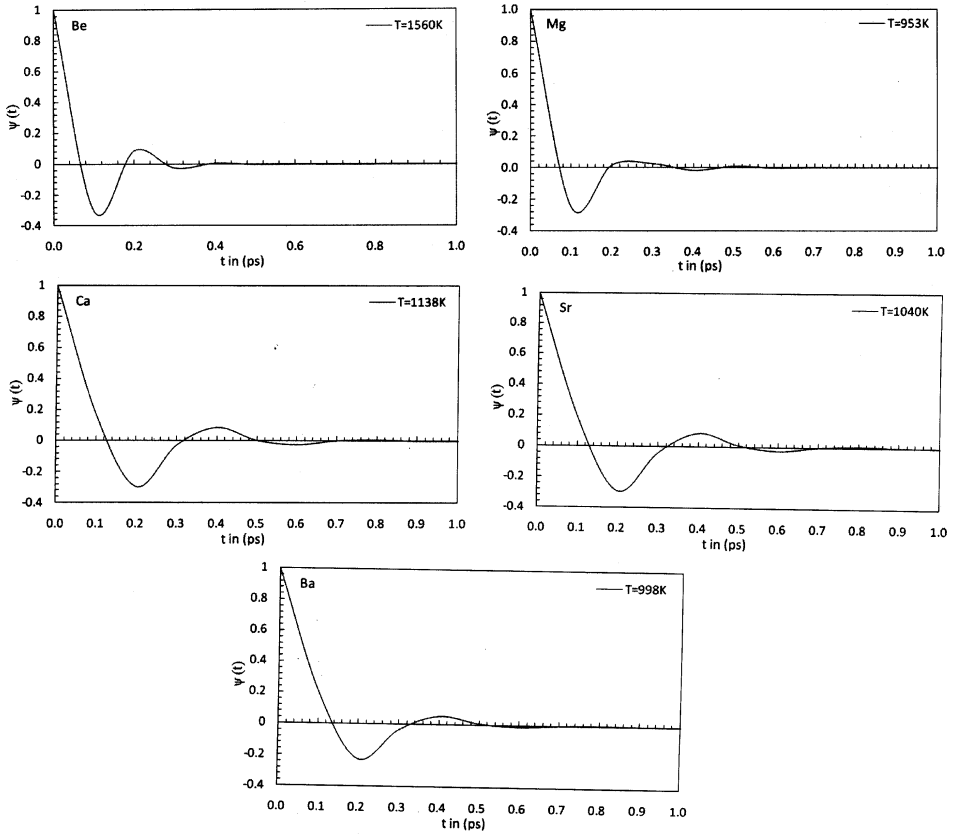

Figure 3. The VACF, $\psi(t)$, for Be, Mg, Ca, Sr and Ba near melting temperature.

number of configurations used in calculating various averages and the shortcomings of the pair potential, and hence the pseudopotential.

The properties of crystalline and liquid phases are found to be adequately modelled by the pseudopotential of Baria and Jani [13–15]. Since the self-diffusion coefficient is very sensitive to the temperature and it is doubled at least at each 400 K, it might be a very accurate test of the potential. Unfortunately, no experimental results are available for alkaline-earth metals and we can only compare our results of D with the existing calculations of Alemany *et al* [12] as shown in table 4.

The static structure does not appear to be very sensitive to it as we can see from the results of $g(r)$ and $S(q)$, both being in very good agreement with experiment. So, for this kind of metals, we have to consider a much more sensitive property, and the self-diffusion coefficient could be this one. Unfortunately, the lack of experimental value prevents definitive conclusions.

To conclude, we have performed molecular dynamics study of liquid alkaline-earth metals with the pseudopotential of Baria and Jani [13–15] in order to check the transferability of the model. Considering that this pseudopotential is exempt

from adjustable parameters, the good quality of our results of the structure factor is a strong argument in favour of the transferability of the pseudopotential from the solid state to the liquid state for alkaline-earth metals as far as the pair potential and the ionic structure are concerned.

Acknowledgement

One of the authors (JKB) is thankful to the University Grants Commission (UGC-WRO, Pune) for providing financial support under the minor research project grant (F. No.: 47-719/08).

References

[1] J B van Zytveld, J E Enderby and E W Collings, *J. Phys. F: Met. Phys.* **2**, 73 (1972)
[2] J B van Zytveld, J E Enderby and E W Collings, *J. Phys. F: Met. Phys.* **3**, 1819 (1973)
[3] Y Waseda, K Yokoyama and K Suzuki, *Philos. Mag.* **30**, 1195 (1974)
[4] S P McAlister, E D Crozier and J F Cochran, *Can. J. Phys.* **52**, 1847 (1974)
[5] S Hiemstra, D Prins, G Gabrielse and J B van Zytveld, *Phys. Chem. Liq.* **6**, 271 (1977)
[6] J G Cook and M J Laubitz, *Can. J. Phys.* **54**, 928 (1976)
[7] G A de Wijs, G Pastore, A Selloni and W van der Lugt, *Phys. Rev. Lett.* **75**, 4480 (1995)
[8] W Jank and J Hafner, *Phys. Rev.* **B42**, 6926 (1990)
[9] V K Ratti and R Evans, *J. Phys. F: Met. Phys.* **3**, L238 (1973)
[10] L E Gonzalez, A Meyer, M P Iniguez, D J Gonzalez and M Silbert, *Phys. Rev.* **E47**, 4120 (1993)
[11] Hong Seok Kang, *Phys. Rev.* **B60**, 6362 (1999)
[12] M M G Alemany, J Casas, C Rey, L E Gonzalez and L J Cal-lego, *Phys. Rev.* **E56**, 6818 (1997)
[13] J K Baria and A R Jani, *Physica* **B328**, 317 (2003)
[14] J K Baria and A R Jani, *Pramana – J. Phys.* **60**, 1235 (2003)
[15] J K Baria and A R Jani, *Physica* **B404**, 2401 (2009)
[16] J-F Wax and J-L Bretonnet, *J. Non-Cryst. Solids* **250–252**, 30 (1999)
[17] S Ichimaru and K Utsumi, *Phys. Rev.* **B24**, 7385 (1981)
[18] M Hasegawa and M Watabe, *J. Phys. Soc. Jpn* **32**, 14 (1972)
[19] D Pines and P Nozieres, *Quantum liquids* (Benjamin, New York, 1966)
[20] Y Waseda, *The structure of noncrystalline materials* (McGraw-Hill, New York, 1980)
[21] J M Haile, *Molecular dynamics simulation: Elementary methods* (Wiley, New York, 1992)
[22] K A Gschneider, *Solid State Phys.* **16**, 275 (1964)
[23] M Shimoji, *Liquid metals* (Academic, London, 1977)
[24] B J Alder and T E Wainwright, *Phys. Rev.* **A1**, 18 (1970)
[25] D Levesque and W T Ashurst, *Phys. Rev. Lett.* **33**, 977 (1972)
[26] U Balucani, A Torcini and R Vallauri, *Phys. Rev.* **A46**, 2159 (1992); *Phys. Rev.* **B47**, 3011 (1993)
[27] N Gupta, K C Jain and N S Saxena, *Phys. Status Solidi* **B165**, 377 (1991)